Int J Adv Manuf Technol (2016) 83:1887–1904
DOI 10.1007/s00170-015-7705-y

ORIGINAL ARTICLE

A new top-down design method for the stiffness of precision machine tools

Yiguang Shi[1] · **Xingyu Zhao**[1] · **Hongjie Zhang**[1,2] · **Yingxin Nie**[3] · **Dawei Zhang**[1]

Received: 24 March 2015 / Accepted: 6 August 2015 / Published online: 21 August 2015

Abstract This work describes a new top-down design method for the stiffness of precision machine tools that considers the entire machine stiffness to guarantee the stiffness requirements in the initial design stage. A stiffness modelling method and a stiffness matching design method are presented to achieve the top-down design of the stiffness. A new stiffness characterisation using the stiffness coefficients for characterising the stiffness of the structural parts and the functional units is proposed. The deformation model of the entire machine is established based on multi-body system theory, and the equations of the stiffness coefficients for the deformations of the components are established based on the simultaneous equations of the static equilibrium equations, the deformation compatibility equations and the physical equations. The three-direction (3D) stiffness model is obtained by substituting the equations into the deformation model that reflects the stiffness characteristics of the machine tool. Thus, the reliability of the stiffness model is verified by experiments. Next, the stiffness matching design is performed to confirm the reasonable stiffness values of the parts based on the stiffness model. The finite element method (FEM) is used to validate the proposed method. The contribution rate of the stiffness of the parts to the stiffness of the entire machine is analysed.

Keywords Stiffness model · Stiffness coefficients · Multi-body system theory · Top-down design · Machine tools

Abbreviations

k_{sx}, k_{sy}, k_{sz}	Stiffness coefficients of the spindle in the X, Y and Z directions
k_{hx}, k_{hy}, k_{hz}	Stiffness coefficients of the head stock in the X, Y and Z directions
$k_{f1x}, k_{f2x}, k_{f3x}, k_{f4x}$	Stiffness coefficients of the moving frame in the X direction
$k_{f1z}, k_{f2z}, k_{f3z}, k_{f4z}$	Stiffness coefficients of the moving frame in the Z direction
$k_{c1y}, k_{c2y}, k_{c3y}, k_{c4y}$	Stiffness coefficients of the column in the Y direction
$k_{c1z}, k_{c2z}, k_{c3z}, k_{c4z}$	Stiffness coefficients of the column in the Z direction
k_{px}, k_{py}, k_{pz}	Stiffness coefficients of the workpiece in the X, Y and Z directions
k_{rx}, k_{ry}, k_{rz}	Stiffness coefficients of the worktable in the X, Y and Z directions
$k_{b1x}, k_{b1y}, k_{b1z}$	Stiffness coefficients of the bed in the X, Y and Z directions
$k_{xgn}, k_{ygn}, k_{zgn}$	Normal stiffness coefficients of the X-, Y- and Z-axis guide way
$k_{xgt}, k_{ygt}, k_{zgt}$	Tangential stiffness coefficients of the X-, Y- and Z-axis guide way
$k_{bsx}, k_{bsx}, k_{bsz}$	Stiffness coefficients of the X-, Y- and Z-axis ball screw
B_y	Distance from the tool tip to the top surface of the bed

✉ Yiguang Shi
syg17@163.com

✉ Dawei Zhang
medzhang@tju.edu.cn

[1] Key Laboratory of Mechanism Theory and Equipment Design of Ministry of Education, Tianjin University, Tianjin 300072, China

[2] School of Mechanical Engineering, Tianjin Polytechnic University, Tianjin 300387, China

[3] Beijing Machine Tool Research Institute, Beijing 101312, China

B_z	Distance from the tool tip to the centre of four guide blocks on the bed
D_c	Distance between the guide blocks on the front surface of the column in the X direction
D_f	Distance between the guide blocks on the front surface of the moving frame in the X direction
L_c	Distance between the guide blocks on the front surface of the column in the Y direction
L_f	Distance between the guide blocks on front surface of moving frame in the Y direction
L_x	Distance between the guide blocks on the bed in the X direction
L_z	Distance between the guide blocks on the bed in the Z direction
R_c	Distance from the column to the tool tip
R_f	Distance from the moving frame to the tool tip
$\Delta x_{01}, \Delta y_{01}, \Delta z_{01}$	Deformations of the bed in the X, Y and Z directions
$\Delta\alpha_{01}, \Delta\beta_{01}, \Delta\gamma_{01}$	Deformations of the bed around the X-, Y- and Z-axis
$\Delta x_{12}, \Delta y_{12} \Delta z_{12}$	Deformations of the worktable in the X, Y and Z directions
$\Delta x_{23}, \Delta y_{23}, \Delta z_{23}$	Deformations of the workpiece in the X, Y and Z directions
$\Delta x_{45}, \Delta z_{45}$	Deformations of the X-axis moving component in the X and Z directions
$\Delta\alpha_{45}, \Delta\beta_{45}$	Deformations of the X-axis moving component around the X- and Y-axis
$\Delta y_{04}, \Delta z_{04}$	Deformations of the column in the X and Z directions
$\Delta\alpha_{04}, \Delta\beta_{04}$	Deformations of the column around the X- and Y-axis
$\Delta x_{56}, \Delta y_{56}, \Delta z_{56}$	Deformations of the Y-axis moving component in the X, Y and Z directions
$\Delta x_{67}, \Delta y_{67}, \Delta z_{67}$	Deformations of the spindle in the X, Y and Z directions
$L^i(j)$ i=0,1,2,3, 4	Lower body operator
$N_{x1}, N_{x2}, N_{x3}, N_{x4}$	Normal forces applied on the moving frame from the force in the X direction
$N_{y1}, N_{y2}, N_{y3}, N_{y4}$	Normal forces applied on the moving frame from the force in the Y direction
$N_{z1}, N_{z2}, N_{z3}, N_{z4}$	Normal forces applied on the moving frame from the force in the Y direction
$Q_{x1}, Q_{x2}, Q_{x2}, Q_{x4}$	Tangential forces applied on the moving frame from the force in the X direction
$1/n_b$, $1/t_b$	Influence factors for the normal and tangential stiffness values of the bed
$1/n_c$, $1/t_c$	Influence factors for the normal and tangential stiffness values of the column
$1/n_f$, $1/t_f$	Influence factors for the normal and tangential stiffness values of the moving frame

1 Introduction

Due to the increasing high requirements of the performance of precision machine tools, more stringent demands in terms of the design are proposed. The increase of the stiffness, one of the important targets of machine tools design, will help improve the efficiency, machining accuracy and surface finish [1]. Studies on the stiffness of machine tools by scholars from various countries are gradually deepening: Dow et al. [2] and Miyaguchi et al. [3] determined the stiffness of small ball end mill using theoretical and experimental methods, as well as its impact on processing quality, the experimental results by Tlusty et al. [4] illustrated the weak stiffness of a spindle-cutting tool system, Ratchev et al. [5, 6] analysed the machining errors caused by the weak stiffness of a workpiece and a cutting tool, Altintas et al. [7] verified that the stiffness of functional units, such as guide ways and ball screws, should not be ignored, and the research results of Salgado et al. [8, 9] indicated that the deformation error calculated using a stiffness model only considers the stiffness of the cutters and the clamping system accounts for 55 % of the experimentally measured error of the entire machine, indicating that the deformation of each component of the machines should be duly considered.

A good stiffness design must use a stiffness model of the entire machine. In view of the aforementioned factors, the existing methods for establishing the stiffness models of entire machines are as follows: Yan et al. [10–12] proposed a semi-analytic method based on a multi-axis system closed-chain stiffness model, which can be utilised to describe the integrated stiffness performance of the entire machining system; Wang et al. [13, 14] established a stiffness matrix of machine tools based on the theory of element stiffness matrix such that the stiffness distribution of the machine tool within a certain work space can be obtained. Huang et al. [15] analysed the stiffness of machine tools using a FEM, from which the impacts of the various components on the stiffness of the entire machine were determined. Portman et al. [16] established the stiffness model of multi-axis machines using the form-shaping function approach.

Those methods involve the modelling and simulation after the construction of a three-dimensional model and focus on the static stiffness analysis of the existing machine tools. Note that stiffness modelling and analysis are performed after the structure design in those methods. They fail to consider the user requirements of the stiffness of the entire machine as the goal and consider the stiffness in the initial design stage.

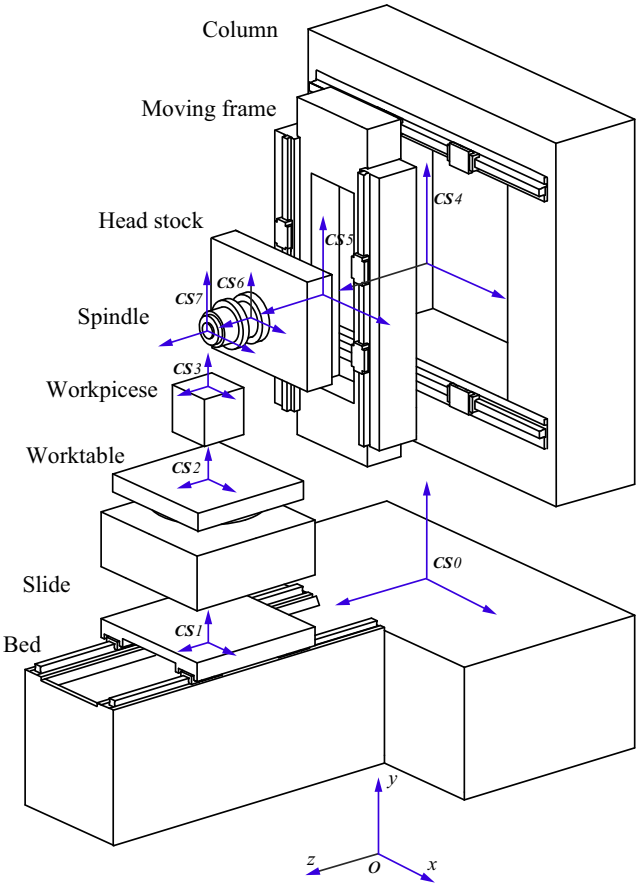

Fig. 1 Schematic diagram of a precision horizontal machining centre of box-in-box construction and the coordinate systems of its components

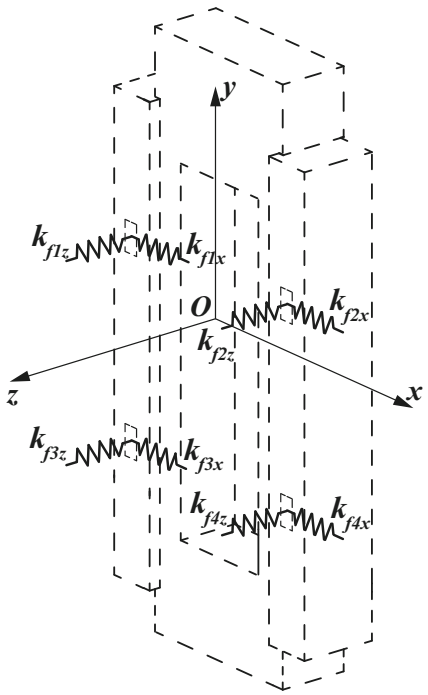

Fig. 2 Stiffness coefficients of the moving frame

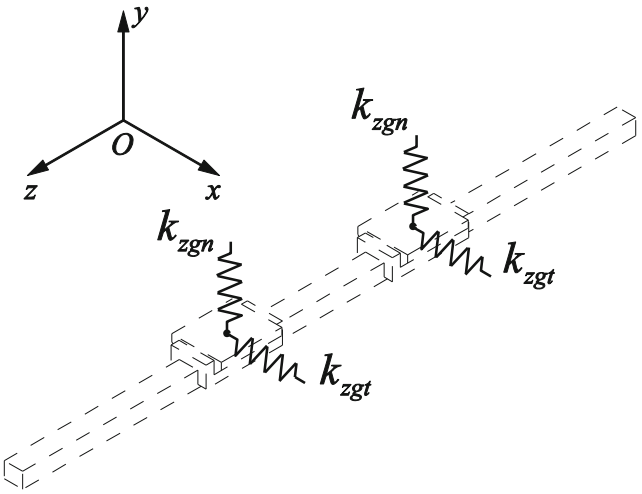

Fig. 3 Stiffness coefficients of the *Z*-axis guide way

Given that, once the requirements cannot be reached, structural modifications must be undertaken repeatedly and passively to achieve the desired goals.

The top-down design method for the stiffness proposed in this paper is a new solution to the above-mentioned problems. The top-down design method is essentially the breaking down of a system to elucidate its compositional sub-systems [17], which mainly includes the conceptual design stage, the skeleton model stage and the detailed design stage [18]. In this study, the skeleton is a vague and incomplete shape of a

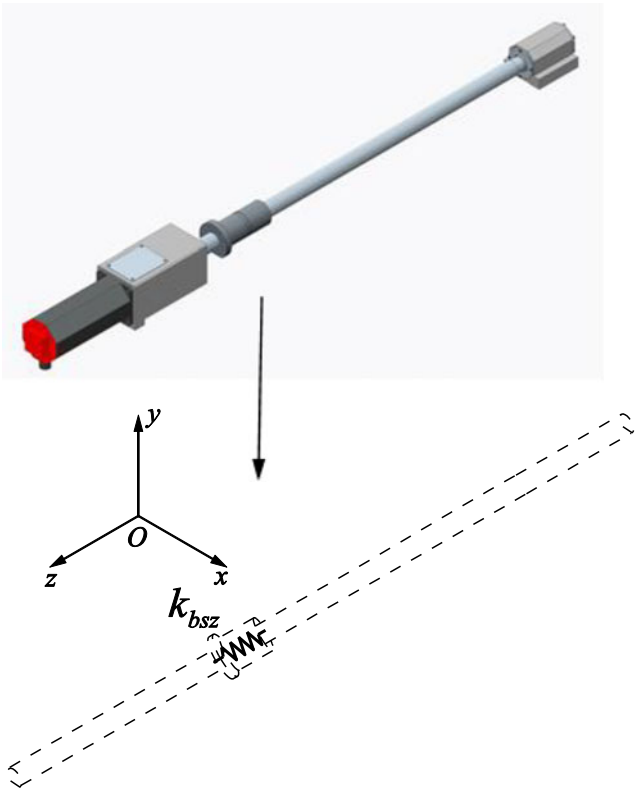

Fig. 4 Stiffness coefficient of the *Z*-axis ball screw

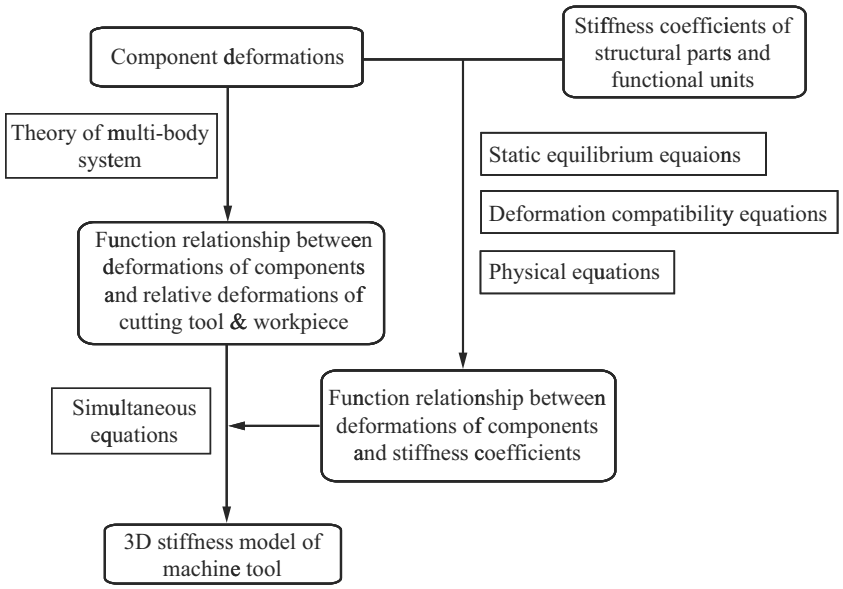

Fig. 5 Illustration of the modelling of the entire machine stiffness

component, which is similar to the concept 'design space' or 'base shape'. The skeleton is often used as an envelope, which constrains the spatial dimension and rough shape of a component [19]. Based on this concept, the process of the top-down design method of stiffness is as follows. First, the stiffness model of the entire machine is established in the skeleton model stage. Next, based on the stiffness model, the stiffness of the entire machine is taken as a target to determine the stiffness of each component reasonably, which can guide the detailed design of each structural part and the model selection of the functional units. According to this design method, the machine tool can meet the stiffness requirements, in the case of only the basic layout dimensions being provided. In addition, the stiffness of each component is allotted precisely, thereby avoiding excessive or insufficient stiffness values of a component.

This paper presents a modelling method of the stiffness of the entire machine and a stiffness matching design method in the skeleton model stage. The structure of the paper is as follows: (1) the abstraction of the stiffness coefficient of each component (could be a part or a sub-assembly), (2) the establishment of the functional relationship between the deformations of the components and the relative deformation of the cutting tool and workpiece according to the multi-body system theory, (3) the force analysis of the structural parts, (4) the establishment of a relationship between the deformation of the components and the stiffness coefficients of the structural parts and the functional units, (5) the stiffness model of the entire machine obtained using the simultaneous equations of the two relationships above, (6) the validation of the stiffness model using an experimental method, (7) the stiffness matching design based on the stiffness model, (8) the validation of the stiffness design method using FEM, and (9) the analysis of contribution rate of the stiffness values of the parts to the stiffness of the entire machine.

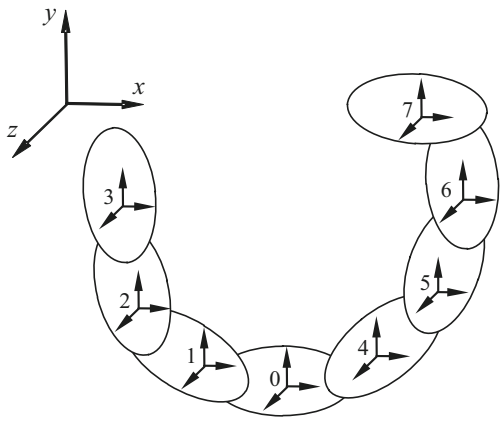

Fig. 6 Topology structure of the machine tool

2 The compositions of the machine tool and their coordinate systems

In the skeleton model stage, the elements of point, line and face are only defined to construct the overall structure placement. In this paper, to illustrate the detailed modelling

Table 1 Lower body array of the machine tool

Typical bodies (j)	1	2	3	4	5	6	7
$L^0(j)$	1	2	3	4	5	6	7
$L^1(j)$	0	1	2	0	4	5	6
$L^2(j)$	0	0	1	0	0	4	5
$L^3(j)$	0	0	0	0	0	0	4
$L^4(j)$	0	0	0	0	0	0	0

Table 2 Characteristic matrices of the machine tool.

Adjacent bodies	Ideal characteristic matrix	Deformation characteristic matrix
0–1	$\mathbf{T}_{01}=\begin{pmatrix}1&0&0&0\\0&1&0&0\\0&0&1&Z_{01}\\0&0&0&1\end{pmatrix}$	$\Delta\mathbf{T}_{01}=\begin{pmatrix}1&-\Delta\gamma_{01}&\Delta\beta_{01}&\Delta x_{01}\\\Delta\gamma_{01}&1&-\Delta\alpha_{01}&\Delta y_{01}\\-\Delta\beta_{01}&\Delta\alpha_{01}&1&\Delta z_{01}\\0&0&0&1\end{pmatrix}$
1–2	$\boldsymbol{T}_{12}=\begin{pmatrix}1&0&0&0\\0&1&0&Y_{12}\\0&0&1&0\\0&0&0&1\end{pmatrix}$	$\Delta\boldsymbol{T}_{12}=\begin{pmatrix}1&0&0&\Delta x_{12}\\0&1&0&\Delta y_{12}\\0&0&1&\Delta z_{12}\\0&0&0&1\end{pmatrix}$
2–3	$\boldsymbol{T}_{23}=\begin{pmatrix}1&0&0&0\\0&1&0&Y_{23}\\0&0&1&0\\0&0&0&1\end{pmatrix}$	$\Delta\boldsymbol{T}_{23}=\begin{pmatrix}1&0&0&\Delta x_{23}\\0&1&0&\Delta y_{23}\\0&0&1&\Delta z_{23}\\0&0&0&1\end{pmatrix}$
0–4	$\boldsymbol{T}_{04}=\begin{pmatrix}1&0&0&0\\0&1&0&Y_{04}\\0&0&1&0\\0&0&0&1\end{pmatrix}$	$\Delta\boldsymbol{T}_{04}=\begin{pmatrix}1&0&\Delta\beta_{04}&0\\0&1&-\Delta\alpha_{04}&\Delta y_{04}\\-\Delta\beta_{04}&\Delta\alpha_{04}&1&\Delta z_{04}\\0&0&0&1\end{pmatrix}$
4–5	$\boldsymbol{T}_{45}=\begin{pmatrix}1&0&0&0\\0&1&0&0\\0&0&1&Z_{45}\\0&0&0&1\end{pmatrix}$	$\Delta\boldsymbol{T}_{45}=\begin{pmatrix}1&0&\Delta\beta_{45}&\Delta x_{45}\\0&1&-\Delta\alpha_{45}&0\\-\Delta\beta_{45}&\Delta\alpha_{45}&1&\Delta z_{45}\\0&0&0&1\end{pmatrix}$
5–6	$\boldsymbol{T}_{56}=\begin{pmatrix}1&0&0&0\\0&1&0&0\\0&0&1&Z_{56}\\0&0&0&1\end{pmatrix}$	$\Delta\boldsymbol{T}_{56}=\begin{pmatrix}1&0&0&\Delta x_{56}\\0&1&0&\Delta y_{56}\\0&0&1&\Delta z_{56}\\0&0&0&1\end{pmatrix}$
6–7	$\boldsymbol{T}_{67}=\begin{pmatrix}1&0&0&0\\0&1&0&0\\0&0&1&Z_{67}\\0&0&0&1\end{pmatrix}$	$\Delta\boldsymbol{T}_{67}=\begin{pmatrix}1&0&0&\Delta x_{67}\\0&1&0&\Delta y_{67}\\0&0&1&\Delta z_{67}\\0&0&0&1\end{pmatrix}$

approach clearly, the machine tool is shown using a solid model. A precision horizontal machining centre of box-in-box construction is used as an example in this paper; its schematic diagram is shown in Fig. 1. The machine tool is composed of the components of bed, column, *X*-axis moving component, *Y*-axis moving component, spindle, *Z*-axis moving component, worktable and workpiece. The *X*-axis moving component consists of a moving frame and an *X*-axis ball screw, the *Y*-axis moving component consists of a head stock and a *Y*-axis ball screw, and the *Z*-axis moving component consists of a slide and a *Z*-axis ball screw. The cutting tool and spindle are considered together. Ball screws of three directions are not presented in the figure. The deformation due to self-weight is not considered here.

The coordinate systems of the components are defined by the right hand rule, as shown in Fig. 1. *CS*0, *CS*1, *CS*2, *CS*3, *CS*4, *CS*5, *CS*6 and *CS*7 denote the coordinate systems fixed with the bed, *Z*-axis moving component, worktable, workpiece, column, *X*-axis moving component, *Y*-axis moving component and spindle, respectively. The origins of *CS*4, *CS*5, *CS*6 and *CS*7 are on the centreline of the spindle. Taking the column as an example, the origin of its coordinate system is the cross point of the spindle centreline and the rectangular region with the *X*-axis guide way's four guide blocks as the four corners. Similarly, the origins of *CS*1, *CS*2 and *CS*3 are on the centreline of the worktable. The origin of *CS*0 is at the intersection of *CS*4's *Y*-axis and *CS*1's *Z*-axis.

3 Concept of the stiffness coefficients

In structural mechanics, the stiffness coefficient is a physical quantity used to describe the elastic deformation of a structure under external force. The stiffness values of structures, such as bar, beam, shell and plate, can be characterised by the stiffness

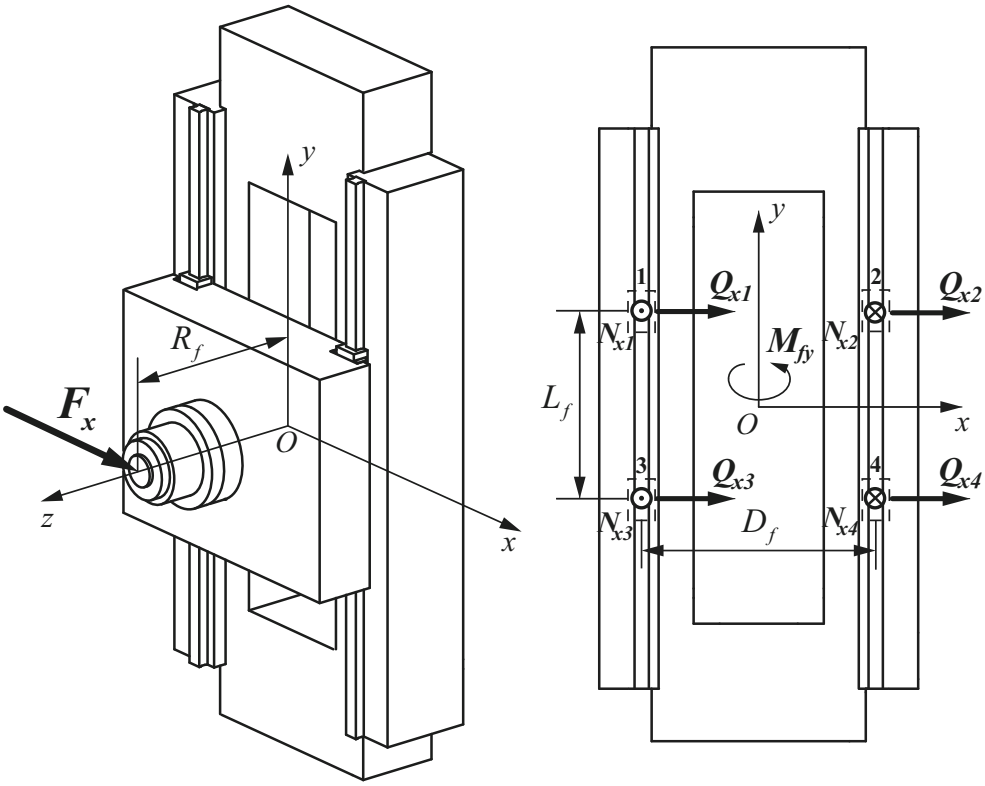

Fig. 7 Dimensions of the moving frame and the force in the *X* direction acted on the moving frame

coefficients of several nodes of these structures. Similarly, the stiffness coefficients of structural parts are used to represent the stiffness of the parts when only their basic dimensions are designed to establish a mathematical model of the entire machine stiffness. The physical meaning of these stiffness coefficients is the stiffness values of several points of structural parts. Deformations of these points should have a direct effect on the relative deformation of the cutting tool and workpiece, and the different magnitudes of deformations of the points should characterise the deformations of the structural parts, such as torsional deformation and bending deformation. In addition, the points can be confirmed in the skeleton model stage. For structures such as column and moving frame, their points are the four points where the four guide blocks are located. Similarly, the point of the head stock is the connection point between the spindle and the head stock. This method has multiple benefits. In early stage of top-down design, the magnitudes of the stiffness coefficients of the structural parts are assigned by the stiffness matching design, and the clarity of the stiffness coefficients makes them become the target for further detailed design of parts. After a concrete model of the structural parts is designed, the magnitudes of the stiffness coefficients are the stiffness values of the corresponding points of the structural parts.

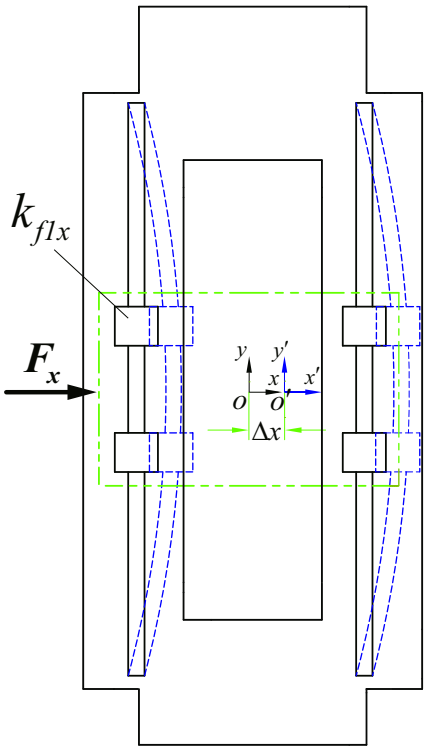

Fig. 8 View of the bending deformation of the moving frame

Considering the moving frame as an example, its stiffness coefficients are $k_{f1x}, k_{f1z}, k_{f2x}, k_{f2z}, k_{f3x}, k_{f3z}, k_{f4x} and k_{f4z}$, which are shown in Fig. 2. Because the *Y*-axis ball screw will withstand a force in the *Y* direction, the moving frame deformation in the *Y* direction is very small. Therefore, the *Y* direction stiffness coefficient of the moving frame cannot be defined. For other structural parts, such as

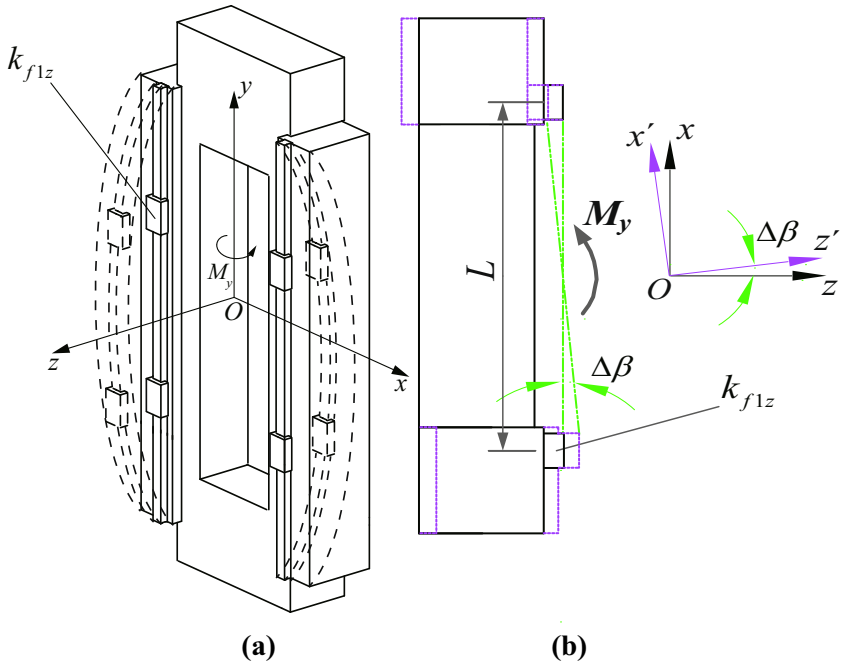

Fig. 9 **a** 3-D view of the torsional deformation of the moving frame. **b** Top view of the torsional deformation of the moving frame

column and headstock, their stiffness coefficients are defined in the same manner.

In the process of stiffness modelling, the functional units are regarded as independent wholes. The stiffness coefficients of these functional units refer to the stiffness of the points where the external force acts and the external force is transmitted from the tool tip [20]. Similar to the structures, the deformations of these points have a direct effect on the relative deformation of the cutting tool and the workpiece. For a spindle, its stiffness coefficients refer to three directions of stiffness of the front of spindle. For guide ways, their stiffness coefficients refer to the normal stiffness and the tangential stiffness of their joints. For example, the stiffness coefficients of the *Z*-axis guide way are shown in Fig. 3. For ball screws, their stiffness coefficients refer to their axial stiffness of the joint of nut and the other parts. For example, the stiffness coefficient of the *Z*-axis ball screw is shown in Fig. 4.

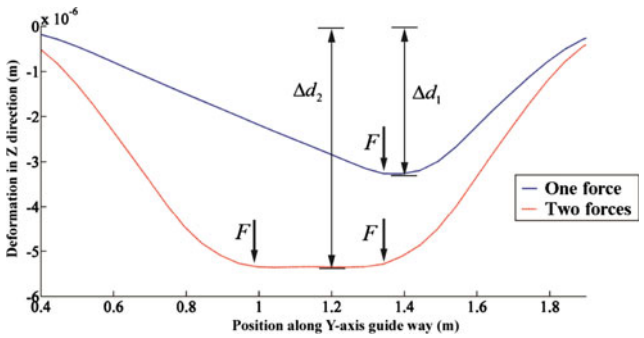

Fig. 10 Deformation curves under the different force conditions

Using the concept of the stiffness coefficient, the stiffness model of the entire machine is established. Illustration of the modelling method is shown in Fig. 5

4 Stiffness modelling

4.1 Deformation modelling

Deformation modelling aims to establish a functional relationship among the deformations of the components and the relative deformations of the cutting tool and workpiece. The theory of a multi-body system is used to describe the topological structure of the machine tool [21–23]. The homogeneous coordinate transformation is used to describe the deformation of the components. The characteristic matrices are established to depict the

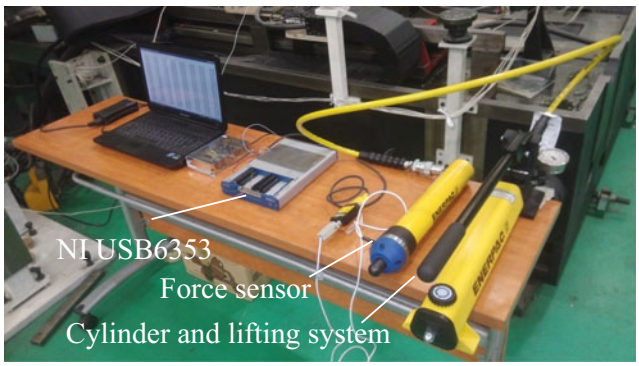

Fig. 11 Experimental setup of a force loading system

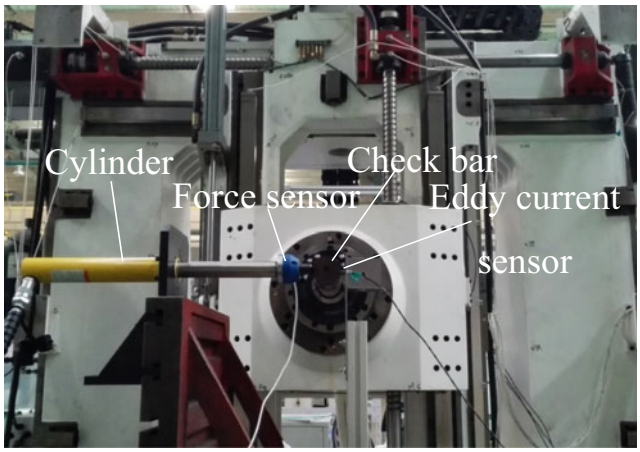

Fig. 12 Experimental setup for the force-displacement measure

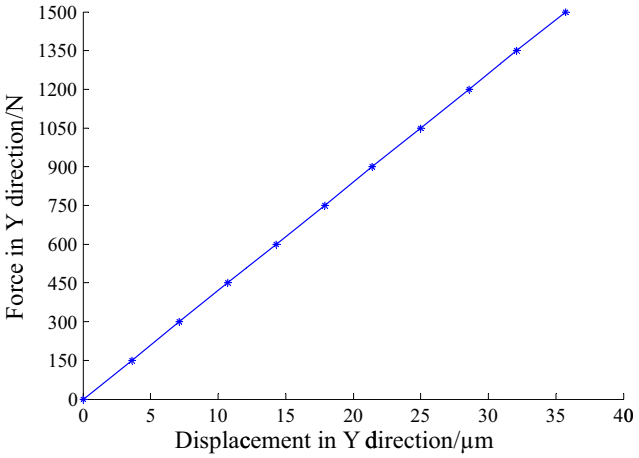

Fig. 14 The curve of force-displacement in *Y* direction

coordinate transformation between adjacent bodies. Finally, as the deviation between the actual position and the theoretical position of a point is analysed, the function relationship will be obtained.

4.1.1 Characteristic matrices of the machine tool

The machine tool can be abstracted into a multi-body system based on its topology structure. On the basis of the theory of a multi-body system, the components of the machine tool are abstracted into some typical bodies, the association of which is described by a topological structure and a lower body array. Figure 6 presents the topology structure, and Table 1 presents the lower body array [24].

The positional relationship between the bodies can be described by the transform of the position matrix of the corresponding coordinate systems in a multi-body system [25]. Therefore, for convenience of analysis, the coordinate systems of components must be determined, as shown in Fig. 1.

Without the cutting force, all components of the machine tool are assumed to be in a relatively static state. In this ideal static situation (no force applied), the homogeneous transformation matrix between a typical body and its adjacent lower body is called the ideal characteristic matrix. When suffering from cutting forces, all the components of the machine tool generate tiny deformations. The homogeneous transformation matrix used to describe the actual deformation of a component is called the deformation characteristic matrix. The ideal and deformation characteristic matrices between the adjacent bodies are presented in Table 2. The moving frame is taken as an example. Z_{45}, which is in its ideal characteristic matrix $\mathbf{T}_{45}$, refers to the distance from the column coordinate system origin to moving frame coordinate system origin. Δx_{45}, Δz_{45}, $\Delta\alpha_{45}$ and $\Delta\beta_{45}$, which are in the deformation characteristic matrix of the moving frame, refer to the deformations of the *X*-axis moving component in the *X* and *Z* directions and around the *X*- and *Y*-axis.

4.1.2 Deformation model

$\boldsymbol{Q}_t(x_t,y_t,z_t)$ is the coordinates of a point in the spindle coordinate system. Using a series of homogeneous coordinate

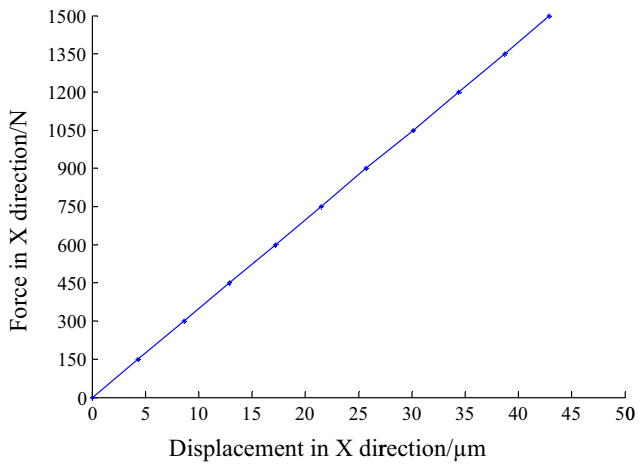

Fig. 13 The curve of force-displacement in *X* direction

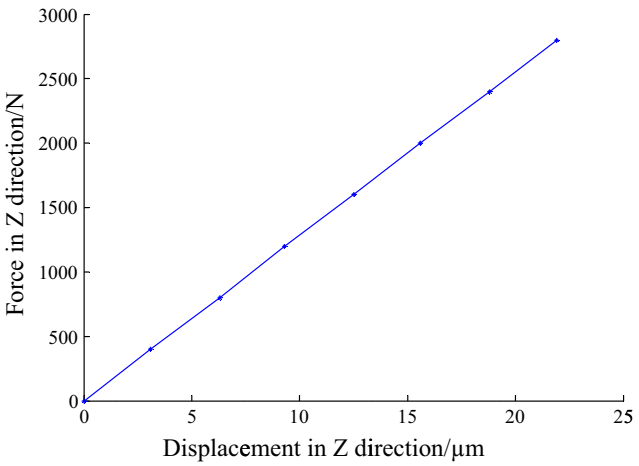

Fig. 15 The curve of force-displacement in *Z* direction

Table 3 Stiffness coefficients of the parts and the functional units

Stiffness coefficients	Values	Stiffness coefficients	Values
k_{sx} ($N/\mu m$)	113	k_{f1z} ($N/\mu m$)	519
k_{sy} ($N/\mu m$)	108	k_{ygn} ($N/\mu m$)	2429
k_{sz} ($N/\mu m$)	530	k_{ygt} ($N/\mu m$)	1395
k_{hx} ($N/\mu m$)	1403	k_{bsx} ($N/\mu m$)	280
k_{hy} ($N/\mu m$)	1525	k_{c1y} ($N/\mu m$)	306
k_{hz} ($N/\mu m$)	4825	k_{c1z} ($N/\mu m$)	201
k_{bsy} ($N/\mu m$)	310	k_{xgn} ($N/\mu m$)	1875
k_{f1x} ($N/\mu m$)	362	k_{xgt} ($N/\mu m$)	1286
k_{bsz} ($N/\mu m$)	430	k_{rx} ($N/\mu m$)	2467
k_{b1x} ($N/\mu m$)	550	k_{ry} ($N/\mu m$)	14740
k_{zgn} ($N/\mu m$)	1875	k_{rz} ($N/\mu m$)	2467
k_{b1y} ($N/\mu m$)	1030	k_{zgt} ($N/\mu m$)	1286

transformation operations of the component coordinate systems, the coordinates can be transformed into the corresponding coordinates in the workpiece coordinate system [26]. If deformation of the components does not occur, then the corresponding coordinate is in a theoretical position $\boldsymbol{Q}_w(x_w,y_w,z_w)$. Thus, the coordinate calculation formula of the theoretical position is obtained as follows:

$$[x_w, y_w, z_w, 1]^T = \boldsymbol{T}_{37}[x_t, y_t, z_t, 1]^T \tag{1}$$

$$\boldsymbol{T}_{37} = \boldsymbol{T}_{67}\boldsymbol{T}_{56}\boldsymbol{T}_{45}\boldsymbol{T}_{04}\boldsymbol{T}_{10}\boldsymbol{T}_{21}\boldsymbol{T}_{32} \tag{2}$$

However, if the components deform due to the cutting force, then the coordinate deviates from the theoretical position to the actual position $\boldsymbol{Q}'_w(x'_w,y'_w,z'_w)$. As a result, the actual position can be calculated:

$$\left[x'_w, y'_w, z'_w, 1\right]^T = \boldsymbol{T}'_{37}[x_t, y_t, z_t, 1]^T \tag{3}$$

$$\boldsymbol{T}'_{37} = \boldsymbol{T}'_{67}\boldsymbol{T}'_{56}\boldsymbol{T}'_{45}\boldsymbol{T}'_{04}\boldsymbol{T}'_{10}\boldsymbol{T}'_{21}\boldsymbol{T}'_{32} \tag{4}$$

where $\boldsymbol{T}'_{ij}$ is an actual characteristic matrix. i and j are the serial numbers of the adjacent bodies. The relationship between $\boldsymbol{T}'_{ij}$ and $\boldsymbol{T}_{ij}$ can be expressed as

$$\boldsymbol{T}'_{ij} = \boldsymbol{T}_{ij}\Delta\boldsymbol{T}_{ij} \tag{5}$$

The deviation between the actual position $\boldsymbol{Q}'_w(x'_w,y'_w,z'_w)$ and the theoretical position $\boldsymbol{Q}_w(x_w,y_w,z_w)$ correspond to the relative deformations of the cutting tool and the workpiece. The deviations Δx, Δy and Δz can be expressed as

$$\begin{pmatrix}\Delta x\\ \Delta y\\ \Delta z\end{pmatrix} = \begin{pmatrix} B_z\Delta\beta_{01} + B_y\Delta\gamma_{01} - \Delta x_{01} - \Delta x_{12} - \Delta x_{23} + \Delta x_{45} + \Delta x_{56} + R_f\Delta\beta_{45} + \Delta x_{67} + R_c\Delta\beta_{04} \\ \Delta y_{56} - R_c\Delta\alpha_{04} - \Delta y_{01} - \Delta y_{12} - \Delta y_{23} - R_f\Delta\alpha_{45} - B_z\Delta\alpha_{01} + \Delta y_{67} + \Delta y_{04} \\ \Delta z_{04} + \Delta z_{45} - \Delta z_{01} - \Delta z_{12} - \Delta z_{23} - B_y\Delta\alpha_{01} + \Delta z_{67} + \Delta z_{56}\end{pmatrix} \tag{6}$$

where

$$B_z = Z_{01} - Z_{45} - Z_{56} - Z_{67}; R_c = Z_{45} + Z_{56} + Z_{67}; B_y = Y_{04}; R_f = Z_{56} + Z_{67}.$$

4.2 Force analysis of the structural parts

By conducting force analysis, the force conditions of the structural parts are obtained when the cutting forces are applied at the tool tip; the results of such an analysis are beneficial for establishing the relationships between the deformations and the stiffness coefficients.

4.2.1 Analysis of the force in the X direction

When a $+X$ direction unit force acts on the tool tip, it is equivalent to a force, $+F_x\vec{i}$, and a moment, $+M_{fy}\vec{k}$, on the moving frame [15]. The moment is equal to a cross product of the distance $+R_f\vec{k}$ and the force $+F_x\vec{i}$, and the moment can be represented by a pair of couples, $\pm\left(M_{fy}/D_f\right)\vec{k}$. Next, the equivalent forces act on areas 1–4 are shown in Fig. 7. Areas 1 and 3 are subjected to a tangential force, $+\left(F_x/4\right)\vec{i}$, and a tensile force, $+\left(F_xR_f/2D_f\right)\vec{k}$. Similarly, areas 2 and 4 are subjected to a tangential force, $+\left(F_x/4\right)\vec{i}$, and a compressive

Table 4 Dimensions of the machine tool

Dimensions	R_f (m)	L_f (m)	D_f (m)	R_c (m)	L_c (m)	D_c (m)	B_z (m)	L_z (m)	B_y (m)	L_x (m)
Values	0.51	0.6	0.68	0.73	1.54	0.84	0.3	0.63	1.19	0.93

Table 5 Factors of influence for the machine tool

Factors of influence	$1/n_f$	$1/t_f$	$1/n_c$	$1/t_c$	$1/n_b$	$1/t_b$
Values	0.6	0.52	0.778	0.54	0.67	0.24

force, $-\left(F_x R_f/2D_f\right)\overrightarrow{k}$. The equivalent forces are obtained as follows:

$$M_{fy}\overrightarrow{j} = R_f\overrightarrow{k} \times F_x\overrightarrow{i} \tag{7}$$

$$M_{fy}\overrightarrow{j} = D_f\overrightarrow{i} \times \left[-\left(\frac{M_{fy}}{D_f}\right)\overrightarrow{k}\right] \tag{8}$$

$$D_f\overrightarrow{i} \times \left[-\left(\frac{M_{fy}}{D_f}\right)\overrightarrow{k}\right] = D_f\overrightarrow{i} \times 2\left[-\left(\frac{F_x R_f}{2D_f}\right)\overrightarrow{k}\right] \tag{9}$$

$$N_{x1}\overrightarrow{k} = N_{x3}\overrightarrow{k} = +\left(\frac{F_x R_f}{2D_f}\right)\overrightarrow{k} \tag{10}$$

$$Q_{x1}\overrightarrow{i} = Q_{x3}\overrightarrow{i} = +\frac{F_x}{4}\overrightarrow{i} \tag{11}$$

$$N_{x2}\overrightarrow{k} = N_{x4}\overrightarrow{k} = -\left(\frac{F_x R_f}{2D_f}\right)\overrightarrow{k} \tag{12}$$

$$Q_{x2}\overrightarrow{i} = Q_{x4}\overrightarrow{i} = +\frac{F_x}{4}\overrightarrow{i} \tag{13}$$

4.2.2 Analysis of the force in the Y direction

When a $+Y$ direction unit force acts on the tool tip, it generates a force, $+F_y\overrightarrow{i}$, which is endured by the *Y*-axis feeding device, and a moment, $-M_{fx}\overrightarrow{i}$, with respect to the moving frame. Because the analysis method is similar to that of the X direction, the equivalent forces of the Y direction are expressed as follows:

$$-M_{fx}\overrightarrow{i} = R_f\overrightarrow{k} \times F_y\overrightarrow{j} \tag{14}$$

$$-M_{fx}\overrightarrow{i} = -L_f\overrightarrow{j} \times \left(\frac{M_{fx}}{L_f}\right)\overrightarrow{k} \tag{15}$$

$$-L_f\overrightarrow{j} \times \left(\frac{M_{fx}}{L_f}\right)\overrightarrow{k} = -L_f\overrightarrow{j} \times 2\left(\frac{F_y R_f}{2L_f}\right)\overrightarrow{k} \tag{16}$$

$$N_{y1}\overrightarrow{k} = N_{y2}\overrightarrow{k} = -\left(\frac{F_y R_f}{2L_f}\right)\overrightarrow{k} \tag{17}$$

Table 6 Experimental results and theoretical results of the stiffness of the machine tool

Stiffness of the machine tool	Experimental results	Theoretical results	Difference rate
k_x ($N/\mu m$)	35	43	18.6 %
k_y ($N/\mu m$)	42	52	19.2 %
k_z ($N/\mu m$)	128	112	14.3 %

Table 7 Basic layout dimensions of the cutting tool loop

Dimensions	R_f (m)	L_f (m)	D_f (m)	R_c (m)	L_c (m)	D_c (m)
Values	0.65	0.56	0.72	0.96	1.42	0.72

$$N_{y3}\overrightarrow{k} = N_{y4}\overrightarrow{k} = +\left(\frac{F_y R_f}{2L_f}\right)\overrightarrow{k} \tag{18}$$

4.2.3 Analysis of the force in the Z direction

When a $-Z$ direction unit force acts on the tool tip, it is decomposed into four forces of the same magnitude applied on areas 1–4. Therefore, each of the four areas is subjected to a compressive force, $-\left(F_z/4\right)\overrightarrow{k}$.

$$N_{z1}\overrightarrow{k} = N_{z2}\overrightarrow{k} = N_{z3}\overrightarrow{k} = N_{z4}\overrightarrow{k} = -\left(\frac{F_z}{4}\right)\overrightarrow{k} \tag{19}$$

4.3 Equations of the stiffness coefficient for deformation

4.3.1 Deformation compatibility and physical equations

As shown in Fig. 8, the moving frame suffers bending deformation under the force in the X direction. Considering the headstock in the middle position, the deformation of the moving frame on each location of the guide block is almost same in the X direction. In other words, k_{f1z}, k_{f2z}, k_{f3z} and k_{f4z} are nearly equal. According to the linear theory of small deformations, the deformations of structural parts can be represented by an offset and rotation of their coordinate systems. Therefore, the deformation of a rectangular region with four guide blocks as four corners can be considered to be rigid body translation, and the amount of the deformation is equal to the coordinate translation of the rigid body. The deformation can be expressed as the ratio of the force exerted on the area to

Table 8 Ranges of stiffness coefficients of the parts via linear programming

Stiffness coefficients	Range	Stiffness coefficients	Range
k_{sx} ($N/\mu m$)	250–370	k_{f1z} ($N/\mu m$)	3000–3704
k_{sy} ($N/\mu m$)	250–370	k_{ygn} ($N/\mu m$)	2000–2439
k_{sz} ($N/\mu m$)	1000–1490	k_{ygt} ($N/\mu m$)	1300–1724
k_{hx} ($N/\mu m$)	3000–4347	k_{bsx} ($N/\mu m$)	250–312
k_{hy} ($N/\mu m$)	3000–4545	k_{c1y} ($N/\mu m$)	2700–3225
k_{hz} ($N/\mu m$)	10000–12048	k_{c1z} ($N/\mu m$)	1000–1300
k_{bsy} ($N/\mu m$)	250–476	k_{xgn} ($N/\mu m$)	1200–1639
k_{f1x} ($N/\mu m$)	1500–1886	k_{xgt} ($N/\mu m$)	1000–1315

Table 9 Factors of influence for the column and moving frame

Factors of influence	$1/n_f$	$1/t_f$	$1/n_c$	$1/t_c$
Values	0.4	0.306	0.867	0.73

the stiffness coefficient of the area:

$$\Delta x = \frac{F_x}{4k_{f1x}} \tag{20}$$

As shown in Fig. 9, the moving frame suffers torsional deformation under the torque around the *Y*-axis. As a result, the upper side of the moving frame is subjected to a compressive force, and the underside of the moving frame is subjected to a tensile force. Thus, the middle position of the upper side produces a deformation in the $-Z$ direction, and the middle position of the underside produces a deformation in the $+Z$ direction, because in the middle position, the deformations of the upper side and the underside can be considered as equal and opposite. Based on the above observations, the deformation of the region can be presented as rigid body rotation, with the amount of the deformation being equal to the coordinate system rotation of the rigid body. Based on the theory of small deformations, the rotation can be expressed as the ratio of the deformation of a guide block area to half of L, which is given as follows:

$$\Delta\beta = \frac{\frac{M_y}{2L}\cdot\frac{1}{k_{f1z}}}{\frac{L}{2}} = \frac{M_y}{k_{f1z}L^2} \tag{21}$$

4.3.2 Deformation synthesis

Based on the basic deformation analysis, the relationship between the deformations of components and the stiffness coefficients of parts can be established.

Table 10 Matched stiffness of the stiffness coefficients of the parts and functional units

Stiffness coefficients	Matched results	Stiffness coefficients	Matched results
k_{sx} ($N/\mu m$)	355	k_{f1z} ($N/\mu m$)	3516
k_{sy} ($N/\mu m$)	367	k_{ygn} ($N/\mu m$)	2350
k_{sz} ($N/\mu m$)	1489	k_{ygt} ($N/\mu m$)	1488
k_{hx} ($N/\mu m$)	3591	k_{bsx} ($N/\mu m$)	310
k_{hy} ($N/\mu m$)	4297	k_{c1y} ($N/\mu m$)	3048
k_{hz} ($N/\mu m$)	11850	k_{c1z} ($N/\mu m$)	1120
k_{bsy} ($N/\mu m$)	471	k_{xgn} ($N/\mu m$)	1601
k_{f1x} ($N/\mu m$)	1676	k_{xgt} ($N/\mu m$)	1247

Taking as an example the *X*-axis moving component, deformations of the *X*-axis moving component contain translations in the *X* direction and *Z* direction and rotations around the *X*- and *Y*-axis. Translation in the *X* direction consists of *X*-axial deformations of the *Y*-axis guide way, *X* axis feed system and the moving frame. Due to the headstock being located in a central position, the deformations of the areas of the four guide blocks are nearly identical. As a result, the translation can be expressed using a deformation of one guide block area. The translation is expressed as follows:

$$\Delta x_{45} = \frac{F_x}{2k_{bsx}} + \frac{F_x}{4k_{f1x}} + \frac{F_x}{4k_{ygt}} \tag{22}$$

Translation in the *Z* direction consists of *Z*-axial deformations of the *Y*-axis guide way and the moving frame. In the same manner as in the *X* direction, the translation in the *Z* direction can be expressed using a deformation of a guide block area as follows:

$$\Delta z_{45} = \frac{-F_z}{4k_{ygn}} + \frac{-F_z}{4k_{f1z}} \tag{23}$$

Rotation around *X*-axis is caused by the moment $-M_{fx}\vec{i}$. From the above force analysis, it is known that areas 1 and 2 are subjected to a compressive force, $-\left(F_yR_f/2L_f\right)\vec{k}$, while areas 3 and 4 are subjected to a tensile force, $+\left(F_yR_f/2L_f\right)\vec{k}$. The rotation can be expressed as follows:

$$\Delta\alpha_{45} = \frac{-\frac{F_yR_f}{2L_f}\left(\frac{1}{k_{f1z}}+\frac{1}{k_{ygn}}\right)}{\frac{L_f}{2}} = -\frac{F_yR_f}{L_f^2}\left(\frac{1}{k_{f1z}}+\frac{1}{k_{ygn}}\right) \tag{24}$$

Rotation around the *Y*-axis is caused by the moment $+M_{fy}\vec{k}$. In the same manner as the rotation around the *X*-axis, the rotation around the *Y*-axis can be expressed as follows:

Table 11 Stiffness coefficients of the structural parts and functional units in the cutting tool loop

Stiffness coefficients	Values	Stiffness coefficients	Values
k_{sx} ($N/\mu m$)	362	k_{f1z} ($N/\mu m$)	3571
k_{sy} ($N/\mu m$)	362	k_{ygn} ($N/\mu m$)	2410
k_{sz} ($N/\mu m$)	1481	k_{ygt} ($N/\mu m$)	1720
k_{hx} ($N/\mu m$)	4310	k_{bsx} ($N/\mu m$)	310
k_{hy} ($N/\mu m$)	4444	k_{c1y} ($N/\mu m$)	3181
k_{hz} ($N/\mu m$)	11,904	k_{c1z} ($N/\mu m$)	1106
k_{bsy} ($N/\mu m$)	470	k_{xgn} ($N/\mu m$)	1620
k_{f1x} ($N/\mu m$)	1865	k_{xgt} ($N/\mu m$)	1310

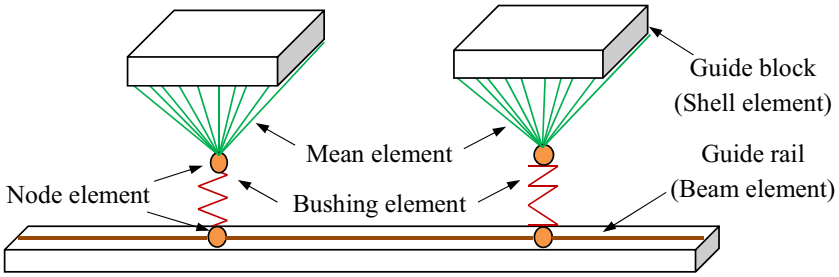

Fig. 16 The finite element model of the guide way

$$\Delta\beta_{45} = \frac{\frac{R_f F_x}{2D_f}\left(\frac{1}{k_{f1z}} + \frac{1}{k_{ygn}}\right)}{\frac{D_f}{2}} = \frac{F_x R_f}{D_f^2}\left(\frac{1}{k_{f1z}} + \frac{1}{k_{ygn}}\right) \tag{25}$$

where

$$\delta_f = \frac{1}{n_f}\frac{F_x R_f}{D_f^2}\left(\frac{1}{k_{f1z}} + \frac{1}{k_{ygn}}\right).$$

$1/n_f$ is the factor of influence about the normal stiffness of the moving frame. The factor of influence is equal to the ratio of the deformation of one guide block location caused by the force acting on another guide block to the deformation caused by the force acting on this guide block directly. The factor of influence is primarily related to the associated dimension. According to the same principle, the modified formulas of all of the deformations of the components can be obtained.

4.3.3 Model correction

In the above analysis, deformations of the structural parts, such as the moving frame, are considered as rigid body translations of the rectangular region with four guide blocks as four corners, and the deformations of the points on the structural parts where the guide blocks located are considered to be independent deformations. However, when two forces are applied on one side of a structural part, which can be considered as a flexible body, the deformations of the adjacent locations affect each other. This phenomenon can be illustrated by the two curves shown in Fig. 10. The blue curve represents the deformation of one side of the moving frame as one guide block location suffers a directional force. The red curve represents the deformation of one side of moving frame as two guide block locations suffer the same directional forces concurrently. Δd_1 and Δd_2 are the maximum deformation values of the two cases represented by the blue and red curves, respectively. From Fig. 8, Δd_2 is smaller than twice the value of Δd_1. Therefore, considering the effect of the force acting upon one area on the deformation of another area, a factor of influence can be added into the formula to represent the effect. For example, the modified expression for $\Delta\beta_{45}$ is as follows:

$$\Delta\beta'_{45} = \frac{F_x R_f}{D_f^2}\left(\frac{1}{k_{f1z}} + \frac{1}{k_{ygn}}\right) + \delta_f = \left(1 + \frac{1}{n_f}\right)\frac{F_x R_f}{D_f^2}\left(\frac{1}{k_{f1z}} + \frac{1}{k_{ygn}}\right) \tag{26}$$

4.4 Stiffness models

The modified formulas are substituted into the functional relationship between the deformations of components and the relative deformations of the cutting tool and the workpiece to obtain the stiffness models. For clarity, the machine tool is divided into the cutting tool loop and the workpiece loop. The cutting tool loop is from the bed to the cutting tool, and the workpiece loop is from the bed to the workpiece. The 3D stiffness models are expressed as follows.

1. Stiffness model of the cutting tool loop:

$$\begin{pmatrix} \frac{1}{k_{tx}} \\ \frac{1}{k_{ty}} \\ \frac{1}{k_{tz}} \end{pmatrix} = \begin{pmatrix} \frac{1}{k_{sx}} + \frac{1}{k_{hx}} + \frac{1}{k'_{fzx}} + \frac{1}{k'_{ygnx}} + \frac{1}{k'_{fxx}} + \frac{1}{k'_{ygtx}} + \frac{1}{k'_{czx}} + \frac{1}{k'_{xgnx}} + \frac{1}{k_{bsx}} \\ \frac{1}{k_{sy}} + \frac{1}{k_{hy}} + \frac{1}{k'_{fzy}} + \frac{1}{k'_{ygny}} + \frac{1}{k_{bsy}} + \frac{1}{k'_{cyy}} + \frac{1}{k'_{xgty}} + \frac{1}{k'_{czy}} + \frac{1}{k'_{xgny}} \\ \frac{1}{k_{sz}} + \frac{1}{k_{hz}} + \frac{1}{k'_{fzz}} + \frac{1}{k'_{ygnz}} + \frac{1}{k'_{czz}} + \frac{1}{k'_{xgnz}} \end{pmatrix} \tag{27}$$

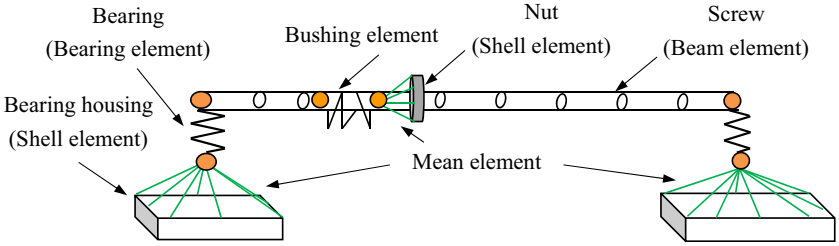

Fig. 17 The finite element model of the ball screw

where

$$\frac{1}{k'_{fzx}}=\left(1+\frac{1}{n_f}\right)\cdot\frac{R_f^2}{D_f^2}\cdot\frac{1}{k_{f1z}};\quad \frac{1}{k'_{ygnx}}=\left(1+\frac{1}{n_f}\right)\cdot\frac{R_f^2}{D_f^2}\cdot\frac{1}{k_{ygn}};\quad \frac{1}{k'_{fxx}}=\left(1+\frac{1}{t_f}\right)\cdot\frac{1}{4}\cdot\frac{1}{k_{f1x}};$$
$$\frac{1}{k'_{ygtx}}=\left(1+\frac{1}{t_f}\right)\cdot\frac{1}{4}\cdot\frac{1}{k_{ygt}};\quad \frac{1}{k'_{czx}}=\left(1-\frac{1}{n_c}\right)\cdot\frac{R_c^2}{D_c^2}\cdot\frac{1}{k_{c1z}};\quad \frac{1}{k'_{xgnx}}=\left(1-\frac{1}{n_c}\right)\cdot\frac{R_c^2}{D_c^2}\cdot\frac{1}{k_{xgn}};$$
$$\frac{1}{k'_{fzy}}=\left(1-\frac{1}{n_f}\right)\cdot\frac{R_f^2}{L_f^2}\cdot\frac{1}{k_{f1z}};\quad \frac{1}{k'_{ygny}}=\left(1-\frac{1}{n_f}\right)\cdot\frac{R_f^2}{L_f^2}\cdot\frac{1}{k_{ygn}};\quad \frac{1}{k'_{cyy}}=\left(1+\frac{1}{t_c}\right)\cdot\frac{1}{4}\cdot\frac{1}{k_{c1y}};$$
$$\frac{1}{k'_{xgty}}=\left(1+\frac{1}{t_c}\right)\cdot\frac{1}{4}\cdot\frac{1}{k_{xgt}};\quad \frac{1}{k'_{czy}}=\left(1+\frac{1}{n_c}\right)\cdot\frac{R_c^2}{L_c^2}\cdot\frac{1}{k_{c1z}};\quad \frac{1}{k'_{xgny}}=\left(1+\frac{1}{n_c}\right)\cdot\frac{R_c^2}{L_c^2}\cdot\frac{1}{k_{xgn}};$$
$$\frac{1}{k'_{fzz}}=\left(1+\frac{1}{n_f}\right)\cdot\frac{1}{4}\cdot\frac{1}{k_{f1z}};\quad \frac{1}{k'_{ygnz}}=\left(1+\frac{1}{n_f}\right)\cdot\frac{1}{4}\cdot\frac{1}{k_{ygn}};\quad \frac{1}{k'_{czz}}=\left(1+\frac{1}{n_c}\right)\cdot\frac{1}{8}\cdot\frac{1}{k_{c1z}};$$
$$\frac{1}{k'_{xgnz}}=\left(1+\frac{1}{n_c}\right)\cdot\frac{1}{8}\cdot\frac{1}{k_{xgn}}.$$

2. Stiffness model of the workpiece loop: where

$$\begin{pmatrix}\frac{1}{k_{wx}}\\ \frac{1}{k_{wy}}\\ \frac{1}{k_{wz}}\end{pmatrix}=\begin{pmatrix}\frac{1}{k_{px}}+\frac{1}{k_{rx}}+\frac{1}{k'_{bxx1}}+\frac{1}{k'_{zgtx1}}+\frac{1}{k'_{byx}}+\frac{1}{k'_{zgnx}}+\frac{1}{k'_{bxx2}}+\frac{1}{k'_{zgtx2}} & & \\ \frac{1}{k_{py}}+\frac{1}{k_{ry}}+\frac{1}{k'_{byy1}}+\frac{1}{k'_{zgny1}}+\frac{1}{k'_{byy2}}+\frac{1}{k'_{zgny2}} & & \\ \frac{1}{k_{pz}}+\frac{1}{k_{rz}}+\frac{1}{k_{bsz}}+\frac{1}{k'_{byz}}+\frac{1}{k'_{zgnz}} & & \end{pmatrix} \tag{28}$$

$$\frac{1}{k'_{bxx1}}=\left(1-\frac{1}{t_b}\right)\cdot\frac{B_z^2}{L_z^2}\cdot\frac{1}{k_{b1x}};\quad \frac{1}{k'_{zgtx1}}=\left(1-\frac{1}{t_b}\right)\cdot\frac{B_z^2}{L_z^2}\cdot\frac{1}{k_{zgt}};\quad \frac{1}{k'_{bxx2}}=\left(1+\frac{1}{n_b}\right)\cdot\frac{B_y^2}{L_x^2}\cdot\frac{1}{k_{b1y}};$$
$$\frac{1}{k'_{zgtx2}}=\left(1+\frac{1}{n_b}\right)\cdot\frac{B_y^2}{L_x^2}\cdot\frac{1}{k_{zgn}};\quad \frac{1}{k'_{bxy1}}=\left(1+\frac{1}{t_b}\right)\cdot\frac{1}{4}\cdot\frac{1}{k_{b1x}};\quad \frac{1}{k'_{zgty1}}=\left(1+\frac{1}{t_b}\right)\cdot\frac{1}{4}\cdot\frac{1}{k_{zgt}};$$
$$\frac{1}{k'_{byy2}}=\left(1+\frac{1}{n_b}\right)\cdot\frac{1}{4}\cdot\frac{1}{k_{b1y}};\quad \frac{1}{k'_{zgny2}}=\left(1+\frac{1}{n_b}\right)\cdot\frac{1}{4}\cdot\frac{1}{k_{zgn}};\quad \frac{1}{k'_{byy1}}=\left(1-\frac{1}{n_b}\right)\cdot\frac{B_z^2}{L_z^2}\cdot\frac{1}{k_{b1y}};$$
$$\frac{1}{k'_{zgny1}}=\left(1-\frac{1}{n_b}\right)\cdot\frac{B_z^2}{L_z^2}\cdot\frac{1}{k_{zgn}};\quad v\frac{1}{k'_{byz}}=\left(1-\frac{1}{n_b}\right)\cdot\frac{B_y^2}{L_z^2}\cdot\frac{1}{k_{b1y}};\quad \frac{1}{k'_{zgnz}}=\left(1-\frac{1}{n_b}\right)\cdot\frac{B_y^2}{L_z^2}\cdot\frac{1}{k_{zgn}}.$$

The stiffness model describes the quantitative relationship of the entire machine stiffness to the stiffness values of the parts and the basic layout dimensions. For example, the X direction stiffness at the tool tip is proportional to the square of the distance between the two guide rails in the same direction and is inversely proportional to the distance between the tool tip and the guide way. Similarly, the Y direction stiffness at the tool tip is proportional to the square of the distance between the two guide blocks on the same guide rail and is inversely proportional to the distance between the tool tip and the guide way.

5 Experimental verifications

To validate the stiffness model, several experimental studies on the stiffness of a horizontal machining centre of box-in-box construction were conducted.

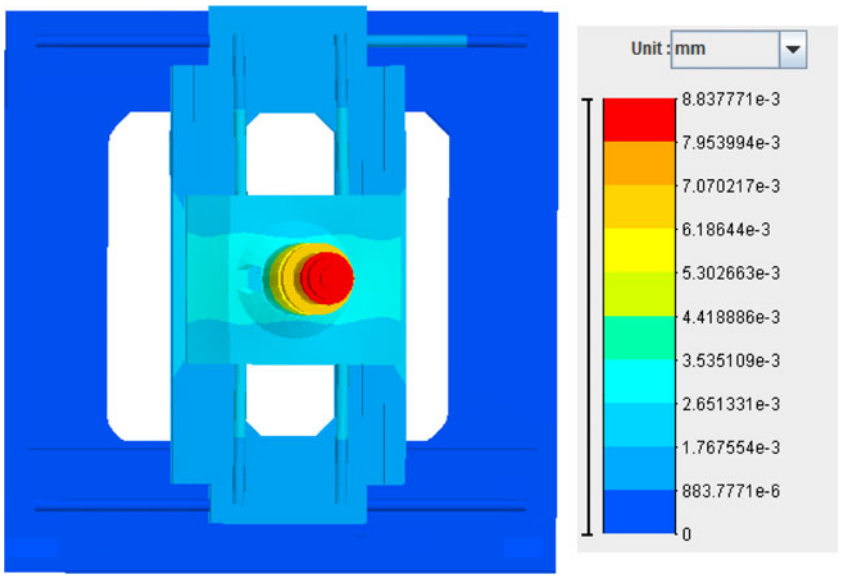

Fig. 18 FEM simulation diagram of the deformation of the cutting tool loop when a 1000-N force in *X* direction is applied on the tool tip

5.1 Experimental procedure

The experimental setup of a force loading system is depicted in Fig. 11. A cylinder and lifting system is used to apply the load. A force sensor, which is installed on the end of the cylinder, is used for collecting force signals. The force signals are conveyed by a D/A converter (NI USB6353) to the host computer.

Experimental principle is shown in Fig. 12. A check bar applied the forces in *X*, *Y* and *Z* directions by the force loading system respectively, and the displacements are measured by the eddy current sensors. The forces and displacements of different directions can be obtained by changing the positions and the installations of the holders. The curves of the loading forces and the deformations are obtained by fitting the measured data, which are shown in Figs. 13, 14 and 15.

5.2 Comparisons between experimental data and theoretical results

To validate the stiffness model, the stiffness coefficients, the factors of influence and the dimensions of the machine tool are substituted into the model. Thus, the stiffness values of the machine tool in *X*, *Y* and *Z* directions can be calculated, which are shown in Table 6. The material of the structural parts is HT250 (elastic modulus $E=1.16\times10^{11}N/m^2$, Poisson's ratio $\mu=0.23$ and density $\rho=7300kg/m^3$). These stiffness coefficients (determined using FEM) are presented in Table 3. Since the functional units are standard units, their stiffness coefficients can be obtained in manuals, which are also presented in Table 3. The dimensions involved are presented in Table 4, and the factors of influence are presented in Table 5. It can be

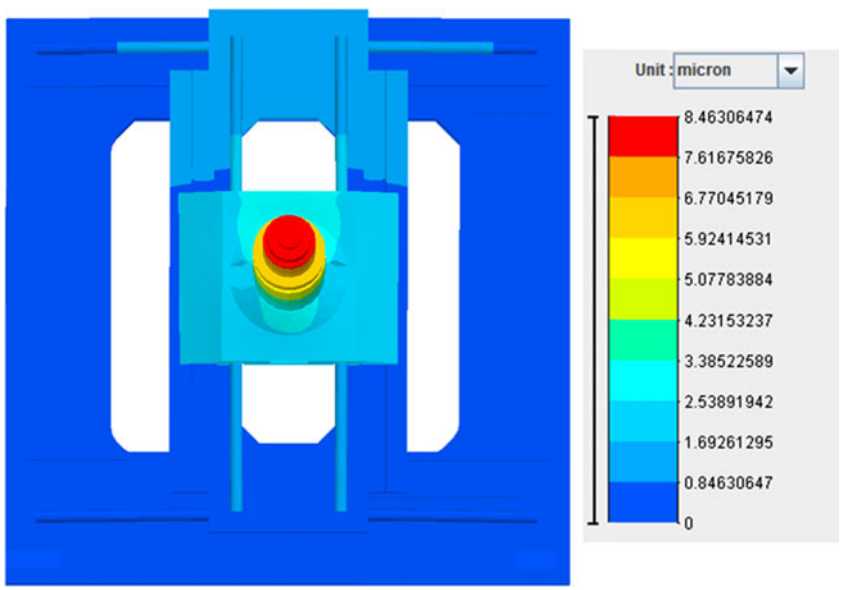

Fig. 19 FEM simulation diagram of the deformation of the cutting tool loop when a 1000-N force in *Y* direction is applied on the tool tip

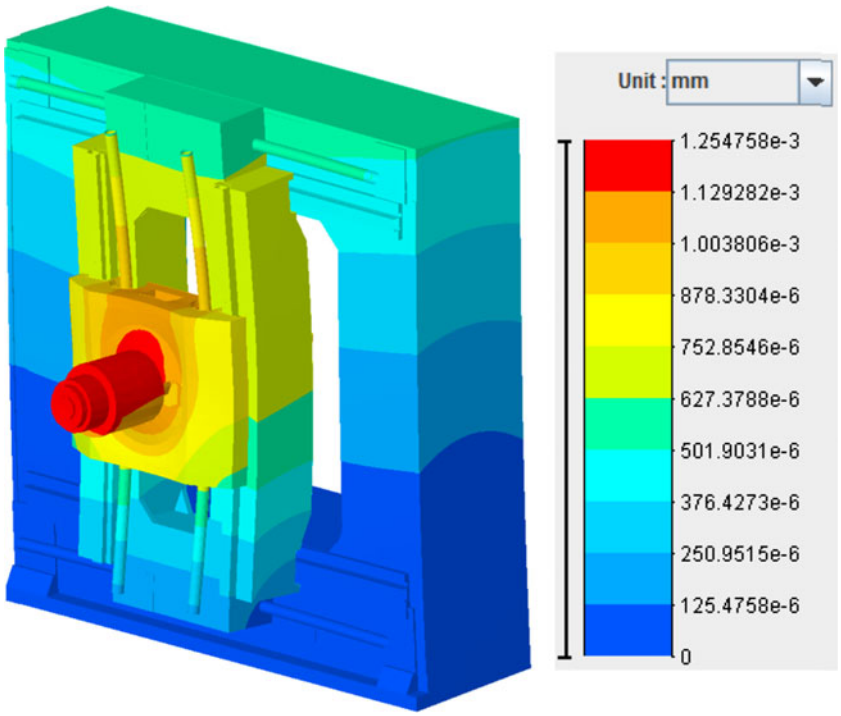

Fig. 20 FEM simulation diagram of the deformation of the cutting tool loop when a 1000-N force in *Z* direction is applied on the tool tip

clarified by Table 6 that the theoretical results are in agreement with the experimental data in the three directions.

6 Stiffness matching design

To achieve the top-down design of the stiffness, the stiffness of the parts should be confirmed as the stiffness of the entire machine determined in the skeleton model stage. Stiffness matching design can be performed based on the stiffness model. The linear programming method is used to realise the stiffness matching design. First, the stiffness model is converted into linear equations, which are considered as constraint equations. Next, reasonable stiffness ranges and the objective function must be selected. Finally, the stiffness of the parts can be obtained using the linear programming method.

Taking the cutting tool loop as an example, the stiffness values in the three directions at the tool tip are given as 125, 135 and 735 N/μm, and the basic dimensions involved are presented in Table 7; these parameters are the given initial conditions. In the stiffness model, the reciprocal of the part stiffness coefficient is set as $x_i(i=1,2,3\cdots)$, and the reciprocal of the stiffness at the tool tip is set as $y_i(i=1,2,3)$. Equation (29) shows the conversion linear equations, which are used as linear constraints in the linear programming. The ranges of stiffness coefficients of the parts are presented in Table 8, and the factors of influence of the column and moving frame are presented in Table 9. These data are obtained from a database that was built based on simulations of similar machines. From Eq. (29), the *Z* direction stiffness of the column has influence on the stiffness values in all three directions at the tool tip. In general, the coefficients of reciprocal of the stiffness are smaller in Eq. (29). As a result, the objective function is to maximise the *Z* direction stiffness of column. Using

Table 12 Given stiffness and FEM results of the stiffness at the tool tip

Stiffness at tool tip	Given stiffness	FEM results	Difference rate
k_{tx} $(N/\mu m)$	125	114	8.8 %
k_{ty} $(N/\mu m)$	135	122	9.6 %
k_{tz} $(N/\mu m)$	735	797	8.4 %

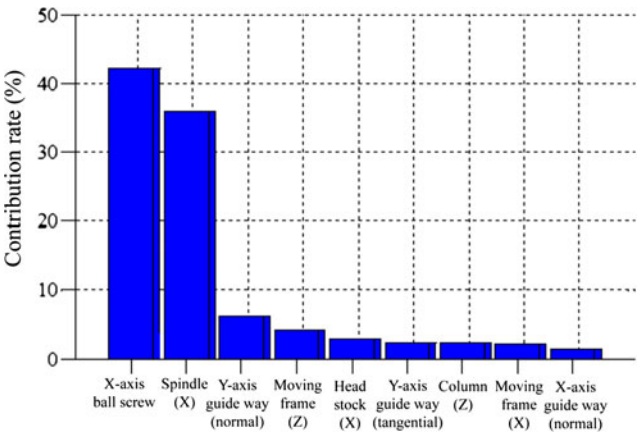

Fig. 21 Contributions of the stiffness of the parts to the *X* direction stiffness at the tool tip

MATLAB™ software, all of the stiffness coefficients of the parts are calculated; the results are presented in Table 10. Thus, aiming at the stiffness of the entire machine, reasonable stiffness values of the parts can be obtained through the stiffness matching design.

$$\begin{cases} y_1 = x_1 + x_4 + 1.1375x_7 + 0.3265x_8 + 0.2467x_{10} + x_{11} + 1.1375x_{13} + 0.3265x_{14} + 0.2467x_{16} \\ y_2 = x_2 + x_5 + 0.797x_7 + 0.4325x_9 + 0.852x_{10} + x_{12} + 0.797x_{13} + 0.4325x_{15} + 0.852x_{16} \\ y_3 = x_3 + x_6 + 0.35x_7 + 0.2338x_{10} + 0.35x_{13} + 0.2338x_{16} \end{cases} \tag{29}$$

where

$$x_1 = \frac{1}{k_{sx}};\quad x_2 = \frac{1}{k_{sy}};\quad x_3 = \frac{1}{k_{sz}};\quad x_4 = \frac{1}{k_{hx}};\quad x_5 = \frac{1}{k_{hx}};\quad x_6 = \frac{1}{k_{hx}}x_7 = \frac{1}{k_{f1z}};\quad x_8 = \frac{1}{k_{f1x}};\quad x_9 = \frac{1}{k_{c1y}};$$
$$x_{10} = \frac{1}{k_{c1z}};\quad x_{11} = \frac{1}{k_{bsx}};\quad x_{12} = \frac{1}{k_{bsy}};\quad x_{13} = \frac{1}{k_{ygn}};\quad x_{14} = \frac{1}{k_{ygt}}\quad x_{15} = \frac{1}{k_{xgt}}\quad x_{16} = \frac{1}{k_{xgn}}.$$

7 Numerical simulation

7.1 Method validation

Based on the matched stiffness of the parts, the initial 3D model of the machine tool can be designed. Consider the cutting tool loop as an illustration. The structural parts are basic-shaped solid bodies, the material of which is ductile iron (elastic modulus $E=1.73\times10^{11}N/m^2$, Poisson's ratio $\mu=0.3$ and density $\rho=7300kg/m^3$). These stiffness coefficients (determined using FEM) are presented in Table 11. Because the functional units are standard units, their stiffness coefficients can be obtained in manuals. For example, the stiffness coefficients of the guide ways and ball screws are found in the NSK handbook; these values are listed in Table 11. Regarded as an assembly, a finite element model of the designed machine tool is built by using SAMCEF™ software. In this finite element model, the guide way model and the ball screw model are created in the manner shown in Figs. 16 and 17. In these models, the node elements come in pairs, and their locations are overlapping. The mean elements are flexible connection elements. Both the bushing elements and the bearing elements can be set using six-dimensional stiffness. The stiffness of the three directions at the tool tip can be calculated using FEM. Figures 18, 19 and 20 show the FEM simulation diagrams of the deformations when a 1000-N force is applied on the tool tip in the *X*, *Y*, and *Z* direction, respectively. The FEM results, the given stiffness and the difference between them are presented in Table 12.

As found in Table 12, the difference rates are limited to 10 %, i.e., the 3D stiffness model and the stiffness design method are credible. In addition, obtaining the stiffness of the parts as the target for structural design, the resulting machine tool is able to meet the requirement of the entire machine stiffness.

7.2 Result analysis

The stiffness model can be used to analyse the contributions of the stiffness values of the parts to stiffness of the entire machine. Such an analysis can enhance the understanding of which stiffness of the parts has more influence on the stiffness on the tool tip. Based upon the data above, the contribution

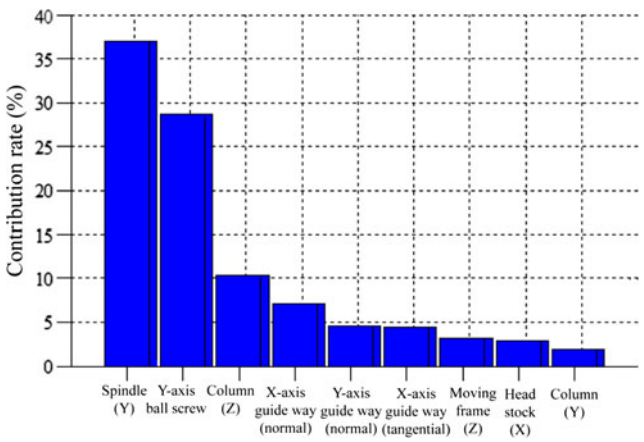

Fig. 22 Contributions of the stiffness of the parts to the *Y* direction stiffness at the tool tip

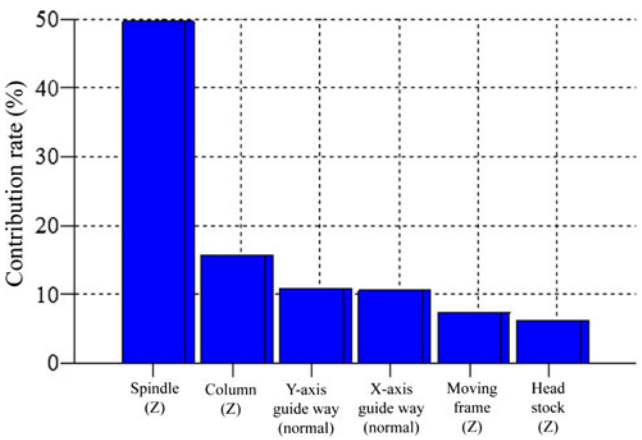

Fig. 23 Contributions of the stiffness of the parts to the *Z* direction stiffness at the tool tip

analysis of the stiffness of parts in the cutting tool loop to the stiffness at the tool tip can be performed.

In this paper, a Design of Experiment (DoE) method, which is a scientific method in studying and treating the relationship between multiple factors and the response variable, is used to analyse the contributions of the parts. In this DoE, the factors and responses are the stiffness coefficients of the parts and the three direction stiffness at the tool tip, respectively. The Optimal Latin Hypercube method is used to establish a design matrix. The number of levers is set to 50. Using the ISIGHT™ software, Pareto Graphs of the three directions can be created. A Pareto Graph shows the effect of a set of factors on a response by plotting the relationship as determined by regression analysis of the data set. The contributions of the stiffness values of the parts to stiffness in the *X*, *Y* and *Z* directions at the tool tip are shown in Figs. 21, 22 and 23, respectively.

The functional units, such as the spindle and the ball screws, are found to have a greater influence on the stiffness in the three directions of the entire machine. Among the stiffness values of the structural parts, the *Z* direction stiffness of the column has a greater impact on the stiffness of the entire machine, especially in the *Y* direction and the *Z* direction. The contributions of other stiffness values of the structural parts are minor.

The contribution analysis synthesises the sensitivity of the stiffness values of the parts to the stiffness of the entire machine. The analysis reveals the effect of the stiffness values of the parts on the stiffness at the tool tip and reflects the stiffness characteristics of the box-in-box construction horizontal machining centre both qualitatively and quantitatively. In addition, the analysis also provides a basis for the detailed design and part structure optimisation.

8 Conclusions

This paper presented a 3D stiffness modelling method and a stiffness matching design for top-down design of the stiffness of precision machine tools in the initial design stage. The following conclusions can be drawn.

1. A new characterisation method for the stiffness of structural parts is proposed. The stiffness coefficients are the stiffness of several points of structural parts, which can be used to represent the stiffness of the parts, and the points are where the four guide blocks located. This method is able to adapt to the design phase in which the machine tool has only the basic layout dimensions. In addition, this method can also abstract the physical model to a mathematical model, which lays the foundation for establishing the entire machine stiffness model.
2. Considering the material flexibility of the parts, the factor of influence is imposed to describe the effect of the force acting upon one point on the deformation of another point. In previous modelling approaches, the deformations of the parts are considered as rigid body translations. The use of an impact factor to modify the stiffness model is more realistic.
3. A 3D stiffness model of a machine tool during the skeleton model stage is established by considering the structural parts and the functional units. The skeleton reflects the stiffness characteristics of the horizontal machining centre with box-in-box construction both qualitatively and quantitatively. The skeleton also shows the effect of the basic dimensions of the machine tool on the entire machine stiffness.
4. Based on the stiffness model, the stiffness matching design is performed. Aiming at stiffness of the entire machine, reasonable stiffness values of the parts can be obtained via the stiffness matching design during the skeleton model stage, which provides a basis for the detailed design of the structural parts and selection of the functional units.
5. Analysis of the contributions of the stiffness values of the parts to the entire machine stiffness is accomplished by using the DoE method. The contribution analysis results revealed the effects of the stiffness values of the structural parts on the stiffness at the tool tip.

This proposed design method has good generality and can be extended to other machines with similar topological structures.

Acknowledgments This research project is supported by a grant from the National Science and Technology Major Project of China (No. 2013ZX04005-013).

References

1. Liu Y, Wang LP, Wang JS (2008) Static Stiffness Research of a Hybrid Machine Tool Based on the Element Stiffness Matrix. China Mech Eng 19(24):2899–2903
2. Dow TA, Miller EL, Garrard K (2004) Tool force and deflection compensation for small milling tools. Precis Eng 28(1):31–45
3. Miyaguchi T, Masuda M, Takeka E, Lwabe H (2001) Effect of tool stiffness upon tool wear in high spindle speed milling using small ball end mill. Precis Eng 25(2):145–154
4. Tlustry J, Ziegert JC, Ridgeway S (2000) A comparison of stiffness characteristics of serial and parallel machine tools. J Manuf Process 2(1):67–76
5. Ratchev S, Liu S, Huang W, Becker AA (2004) A flexible force model for end milling of low rigidity parts. J Mater Process Technol 153:134–138
6. Ratchev S, Liu S, Huang W, Becker AA (2006) An advanced FEA based force induced error compensation strategy in milling. Int J Mach Tools Manuf 46(5):542–551
7. Altintas Y, Verl A, Brecher C, Uriarte L (2011) Machine tool feed drives. CIRP Ann-Manuf Technol 60(2):779–796

8. Salgado MA, De Lacalle LNL, Lamikiz A, Muñoa J, Sánchez JA (2005) Evaluation of the stiffness chain on the deflection of end-mills under cutting force. Int J Mach Tools Manuf 46(6):727–739
9. Olvera D, De Lacalle LNL, Compeán FI, Fz-Valdivielso A, Lamikiz A, Campa FJ (2012) Analysis of the tool tip radial stiffness of turn-milling centers. Int J Adv Manuf Technol 60(9–12):883–891
10. Peng FY, Yan R, Chen W, Yang JZ, Li B (2012) Anisotropic force ellipsoid based multi-axis motion optimization of machine tools. Chin J Mech Eng 25(5):960–967
11. Yan R, Chen W, Peng FY (2012) Closed-loop stiffness modeling and stiffness index analysis of multi-axis machining system. Chin J Mech Eng 48(1):177–184
12. Yan R, Peng FY, Li B (2008) A method of general stiffness modeling for multi-axis machine tool. Intell Robotics Appl 53(15):1013–1021
13. Wu J, Wang JS, Wang LP, Li TM, You Z (2009) Study on the stiffness of a 5-DOF hybrid machine tool with actuation redundancy. Mech Mach Theory 44(2):289–305
14. Lv YN, Wang LP, Guan LW (2008) Stiffness analysis and optimization of a hybrid machine tool based on the stiffness matrix. J Tsinghua Univ (Science and Technology) 48(2):180–183
15. Huang DT-Y, Lee J-J (2001) On obtaining machine tool stiffness by CAE techniques. Int J Mach Tools Manuf 41(8):1149–1163
16. Portman VT, Shneor Y, Chapsky VS, Shapiro A (2014) Form-shaping function theory expansion: stiffness model of multi-axis machines. Int J Adv Manuf Technol 76(5–8):1063–1078
17. Mantyla M (1990) A modeling system for top-down design of assembled products. IBM J Res Dev 34(5):636–659
18. Gao SM, Zhang ST, Chen X, Yang YD (2013) A framework for collaborative top-down assembly design. Comput Ind 64(8):967–983
19. Chen X, Gao SM, Yang YD, Zhang ST (2013) Multi-level assembly model for top-down design of mechanical products. Comput Aided Des 44(10):1033–1048
20. Altintas Y, Brecher C, Weck M, Witt S (2005) Virtual Machine Tool. CIRP Ann-Manuf Technol 54(2):651–674
21. Chen GD, Liang YC, Sun YZ, Chen WQ, Wang B (2013) Volumetric error modeling and sensitivity analysis for designing a five-axis ultra-precision machine tool. Int J Adv Manuf Technol 68(9–12):2525–2534
22. Khan AW, Chen WY (2011) A methodology for systematic geometric error compensation in five-axis machine tools. Int J Adv Manuf Technol 53(5–8):615–628
23. Chen GS, Mei XS, Li HL (2013) Geometric error modeling and compensation for large-scale grinding machine tools with multi-axes. Int J Adv Manuf Technol 69(9–12):2583–2592
24. Su SP, Li SY, Wang GL (2002) Identification method for errors of machining center based on volumetric error model. Chin J Mech Eng 38(7):121–125
25. Liu ZF, Liu GB, Cheng Q, Xuan DS, Chang WF (2012) An identification approach for key geometric error sources of machine tool based on sensitivity analysis. Chin J Mech Eng 48(7):171–179
26. Huang Q, Zhang GB, Zhang XY (2009) Sensitivity analysis of the pose error of machine tool. Chin J Mech Eng 45(6):141–146